**HINDAS - Work Package 5 - Deliverable D15**

# Comparison of experimental neutron production on thin targets with the predictions of widely used high-energy models

S. Leray[1)], J. Cugnon[2)], D. Filges[3)], F. Goldenbaum[3)], J.F. Lecolley[4)] and X. Ledoux[5)]

[1)] *CEA/SPhN, CEA/Saclay, F-91191 Gif-sur-Yvette, Cedex, France,*

[2)] *Université de Liège, Institut de Physique B5, Sart Tilman, B-4000 LIEGE 1, Belgium,*

[3)] *Forschungszentrum Jülich GmbH, Institut für Kernphysik, D-52425 Jülich, Germany,*

[4)] *LPC, 6 Bd du Maréchal Juin, 14050 Caen CEDEX, France,*

[5)] *CEA/SPN, BP 12, F-91680 Bruyères-le-Châtel, France,*

**Abstract**

Comparisons of both the NESSI neutron multiplicities and the double-differential cross-sections measured at SATURNE with predictions of different models widely used in high-energy transport codes are presented. The main conclusion is that the combination of the Bertini intra-nuclear cascade with the Dresner-Atchison evaporation-fission models used with the default options in LAHET shows serious deficiencies, especially at high incident energies. These are due mainly to an overprediction of the excitation energy by the Bertini model at the end of the first stage of the reaction. On the contrary, it is found that the use of the Cugnon intra-nuclear cascade model, INCL2, is able to fairly reproduce the whole bulk of both NESSI and SATURNE results. However, this model still suffers from some defects mostly due to the fact this it does not treat correctly the diffuseness of the nuclear surface. This should be solved in the new version, INCL4, under progress in WP8.

# 1 Introduction

In accelerator-driven sub-critical reactors, which are envisaged for the transmutation of long-lived nuclear waste, a spallation target bombarded by a high intensity proton beam provides the source neutrons that will be multiplied in the sub-critical core. It is therefore of major importance to search for the most efficient conversion of the primary beam energy into neutron production, that means to know precisely the number of neutrons produced in spallation reactions. Also essential is the knowledge of the source neutron energy and spatial distributions for the neutronics of the sub-critical core. Because a fraction of the produced

neutrons have energies much larger than what is usual in a fission or even a fusion reactor, further damages are expected in the structure materials and increased shielding against the neutrons escaping from the system has to be foreseen. Again, a correct assessment of these constraints requires a good prediction of the source neutron properties.

Simulation code packages exist, which make it possible for spallation source designers to predict any of the above mentioned quantities. They generally consist of the coupling of a high-energy transport code, which handles the transport and interactions of the incoming proton and all the produced particles down to 20 (or when possible 150) MeV for neutrons and to stopping for other particles, and a low-energy neutron transport code utilizing evaluated nuclear data files below 20 (150) MeV. The 150 MeV extended data libraries will be provided by WP7 at the end of the HINDAS project. In the high-energy transport codes, the elementary cross-sections are calculated by nuclear physics models. Since the source neutrons are generated and their properties determined by high-energy reactions, it is crucial that the nuclear models be reliable enough, that is, provide correct elementary cross-sections validated on an extensive set of experimental data.

One of the goals of the workpackage 5 of HINDAS was precisely to collect thin target data on both neutron multiplicities (by the NESSI collaboration) and double-differential (p,xn) cross-sections (measured at SATURNE) which could serve as benchmark data for the high-energy nuclear models. These data have been delivered as D9. The second goal was to compare them with the predictions of the models commonly used within high-energy transport codes, in order to assess their possible deficiencies, deficiencies that should be cured in the models developed in the workpackage 8. This is the subject of this report, which actually summarizes and makes the synthesis of more detailed papers on the SATURNE [1, 2] and NESSI [3, 4] results.

# 2 High-energy models used for the comparison

Generally a spallation reaction is modeled as a two step process: a first fast stage, the Intra-Nuclear Cascade (INC), in which the hadron-nucleus interaction consists in a sequence of independent collisions between the incoming particles and nucleons of the target nucleus, leading to an excited residue. It is followed by a second slower stage of de-excitation through particle evaporation, sometimes competing for heavy residues with fission. Some authors introduce a pre-equilibrium step between INC and decay.

Most of the high-energy Monte-Carlo transport codes used for ADS simulations actually

originate from the same source, the HETC code from Oak Ridge [5]. This is the case of the different code packages used in this report, the Jülich HERMES [6, 7] package, the Los Alamos Code System (LAHET) [8] and the TIERCE code from Bruyères-le-Châtel [9]. In all these codes, the default, and consequently the most widely used, models are the Bertini [10] INC and the Dresner evaporation [11], usually associated with the Atchison [12] fission model. However, other more recent INC models are available, for instance the ISABEL [13] model in LAHET and the Cugnon INCL2 [14] model, in HERMES and TIERCE. For evaporation-fission, in these codes, no alternative model is proposed but the codes differ by the choice of the parameters (for instance of the level density parameter or the Coulomb barriers for charged particle evaporation).

Most of the neutrons produced in spallation reactions are emitted during the evaporation process. However, their number is principally determined by the excitation energy $E^*$ left in the target at the end of the cascade process. Indeed, the mean number of evaporated neutrons is given, in the Weisskopf-Ewing model, by

$$\langle n \rangle_{evap} \approx \frac{\bar{E^*}}{S_n + 2\bar{T}}, \tag{1}$$

where $S_n$ is the mean neutron separation energy and $\bar{T}$ is the mean temperature. Roughly speaking, $\bar{T} = \sqrt{\bar{E^*}/a}$, where $a$ is the level density parameter. For average excitation energies considered here, $\bar{T}$ is less than 2-3 MeV, and therefore the number of the evaporated neutrons is not very sensitive to the details of the evaporation models, which enter here essentially through the parameter $a$ only. This means that the number of emitted neutrons should be more sensitive to the choice of the INC than of the evaporation model. This is why in this report more emphasis is put on comparisons of data with different INC models using the same Dresner-Atchison evaporation-fission model. However, we also report on the influence of parameters of the evaporation model on some of the results.

Three INC models are considered in this report, i.e. Bertini [10], ISABEL [13] and INCL2 [14], which have general common features:
- nucleons follow linear trajectories between collisions,
- target Fermi motion is taken into account,
- free nucleon-nucleon cross-sections are used,
- inelastic N-N collisions involving excitation of the Delta-resonance and the creation of pions are included,
- Pauli blocking inhibits collisions leading to already occupied states.

The main differences appear in the treatment of the propagation of the cascade. In

Bertini and ISABEL models, the nucleus is a continuous medium in which the incident particle collides according to its mean free path with a nucleon. This nucleon is then set into motion and can undergo further collisions. In the INCL2 code, all the nucleons are moving according to an initial Fermi distribution and collide as soon as they reach their minimum distance of approach or are reflected on the wall of the nuclear potential. The cascade propagation is followed as a function of time in INCL2 and ISABEL but not in Bertini model. The criterium for stopping the INC is also different. In Bertini and ISABEL, the cascade is stopped when all the particle energies are below a cut-off value while in the INCL2 code a time has been fixed that corresponds approximately to the reaching of thermalization. The description of the diffuseness of the nuclear surface is also different in each model: the nuclear density distribution is described by 3 (resp. 16) different regions in Bertini (resp. ISABEL) while it has a sharp surface in INCL2. Finally, the Pauli blocking is handled differently: in the Bertini model, all collisions leading to a particle momentum below the Fermi level is forbidden, irrespective of the progressive depletion of the Fermi sea during the process. In the two other models, attempt is made to take into account the real occupation rate. In the INCL2 model, for instance, this is done statistically by allowing the collision of two nucleons with a probability equal to the occupation rate in a small phase space volume around the nucleons.

# 3 SATURNE data

## 3.1 Double-differential cross-sections

In this section, the neutron production double-differential cross-sections measured at the SATURNE synchrotron induced by 0.8, 1.2 and 1.6 GeV protons impinging on different targets are compared to different intra-nuclear cascade models implemented into high-energy transport codes. Actually, the targets were a few centimeter thick but can be considered as thin since the rate of secondary reactions is small enough. In fact, secondary reactions contribute for about 10% to the total neutron production but mainly below 2 MeV that is below the detection threshold. These data have been delivered as D9, the Pb data having already been reported on in the Concerted Action FI4I-CT-98-0017, and published in [1, 2] which include the comparison with models summarized in this section.

The high energy part of the neutron spectra allows to directly probe the INC models. Low energy neutrons, which are the majority of the neutrons produced in spallation reactions, are emitted during the evaporation process. However, as already stated, their number mainly depends upon the INC stage since the cascade determines the initial excitation energy of the decaying hot residue and, therefore, the number of evaporated particles. Calculations

have been done using different INC models implemented into high-energy transport codes (in which the actual thickness and diameter of the targets have been taken into account), using always the same Dresner-Atchison evaporation-fission model with the default parameters, for instance the GCCI level density parameterization (see sect. 4.2). INCL2 model does not predict a correct total reaction cross-section mainly because the diffuseness of the nuclear surface is not taken into account. Therefore, the INCL2 calculations were renormalized to the total reaction cross-sections given by the Bertini model which appears to be in very good agreement with experimental values.

In [1], for lead, calculations were performed with the TIERCE [9] code system developed at Bruyères-le-Châtel using either the Bertini or the Cugnon INCL2 model with the same evaporation-fission model (based on Dresner-Atchison model). It was shown that, at the three measured energies, the Bertini model was largely overpredicting the experimental data while INCL2 was giving a rather good agreement. This was ascribed to the higher excitation energy, $E^*$, obtained at the end of the cascade stage with the Bertini calculation than with INCL2 (see sect. 4.4). Several reasons were invoked to explain the difference in $E^*$ between both models : first, INCL2 produces more pions than Bertini. However, the difference in average $E^*$ due to the energy carried away by the pions is only around 30 MeV. Second, it seems that the cut-off energy stopping criterium of Bertini leads to a larger excitation energy than the thermalization time in INCL2. Third, as mentioned in [1], the Pauli blocking is treated in a different way. In Bertini, only collisions of nucleons with momentum larger than the Fermi momentum are allowed while, in INCL2, the actual phase space occupation rate is taken into account. This leads to a less stringent condition, therefore more cascade particles can escape and make the energy remaining in the nucleus lower.

In the LAHET code system [8] it is possible to add after the intra-nuclear cascade stage a pre-equilibrium stage which is expected to reduce the excitation energy of the nucleus by emission of intermediate energy particles prior to the evaporation. Besides, this is also the option recommended by LAHET authors [15]. Also available is the ISABEL model which can be used only up to 1 GeV. Here, we show calculations performed with both models with the same Dresner-Atchison evaporation-fission at 800 MeV for the Pb and Fe target. In the following, Bertini plus pre-equilibrium will be referred to as BPQ. Fig. 1 presents the calculated neutron spectra compared to the experimental data. It can be observed that, for Pb, the BPQ calculation reproduces very well the data, except at very forward angles and high neutron energies where the peak corresponding to the excitation of the $\Delta$ resonance appears much too high. This is a deficiency of Bertini INC model, already pointed out in [16] as due to a bad parameterization of the $NN \rightarrow N\Delta$ reaction angular distribution.

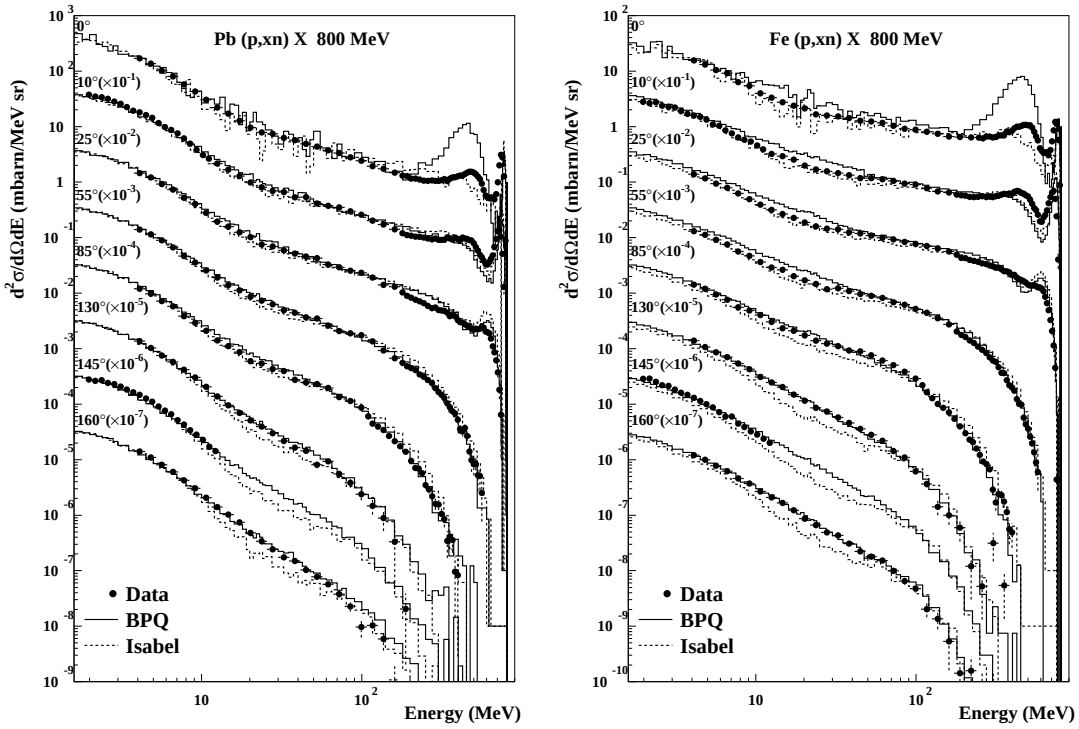


**Figure** 1: *Experimental p (800 MeV) + Pb (left) and Fe (right) neutron double-differential cross-sections compared with calculations performed with LAHET using either Bertini plus pre-equilibrium (solid line) or ISABEL (dashed line) INC model. From [2].*

The problem does not exist with ISABEL nor INCL2 (not shown here). In fact, the three models correctly predict the low energy part of the spectra. This can be understood by the respective excitation energy distributions which were found in [2] to be rather similar at this incident energy. The high energy neutrons beyond 85° are well reproduced by both ISABEL and BPQ calculations but ISABEL underestimates cross-sections at backward angles in the intermediate energy region. For iron, ISABEL presents the same features as for lead while BPQ now overpredicts low and intermediate energy neutron production at forward angles, indicating that the angular distribution of pre-equilibrium neutrons is probably too much forward-peaked.

At 1200 MeV, the use of ISABEL in LAHET being limited to 1 GeV, we compare the data with only BPQ and INCL2 calculations in fig. 2, for Pb and Fe targets. We also performed calculations, which are not shown here, using Bertini without pre-quilibrium. Whatever the target, this model yields too many low energy neutrons, emphasizing that it leads to too high excitation energies. For Pb, both BPQ and INCL2 models give a reasonable agreement with the data, although BPQ tends to slightly overestimates the production of intermediate energies neutrons. As the target becomes lighter, this trend is amplified and BPQ begins

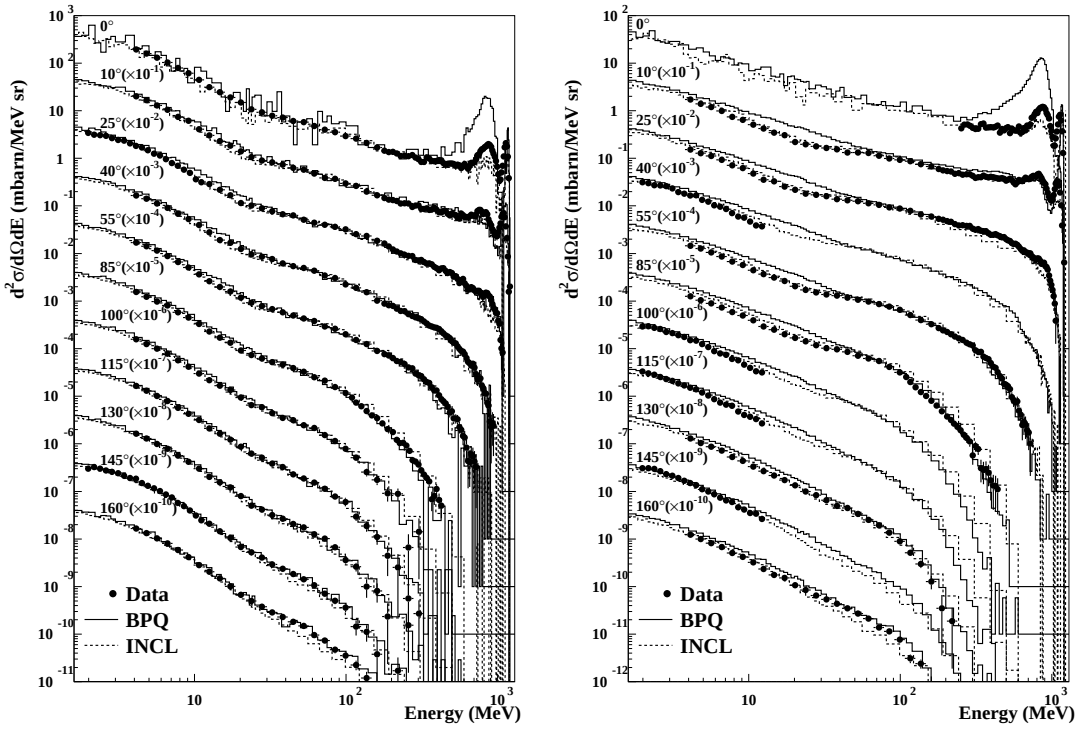


**Figure** 2: *Experimental p (1200 MeV) + Pb (left) and Fe (right) neutron double-differential cross-sections compared with calculations performed using either Bertini plus pre-equilibrium in LAHET (solid line) or INCL2 in TIERCE (dashed line) code. From [2].*

to also overpredict low energy cross-sections. This is an indication that the addition of a pre-quilibrium stage after INC to decrease the too large excitation energy found in Bertini may not be the proper solution: in fact, it seems difficult to obtain the correct evaporation neutron cross-sections without overestimating intermediate energy, i.e. produced by pre-equilibrium, ones. On the contrary, INCL2 reproduces quite well the data for all the targets, proving that the model has a correct mass dependence. Only for the Fe targets at very backward angles, the high energy neutron production is underpredicted.

At 1600 MeV, fig. 3 displays the results for the Pb and Fe targets. For BPQ the tendencies noticed at 1200 MeV are growing worse: even for Pb, the agreement is not very good between 10 and 40 MeV. Since the high energy part of the spectra is always rather well reproduced (except at 0°), this seems to point out a wrong dependence of the pre-equilibrium emission with incident energy. Here again, INCL2 gives a satisfactory agreement with the data for both targets.

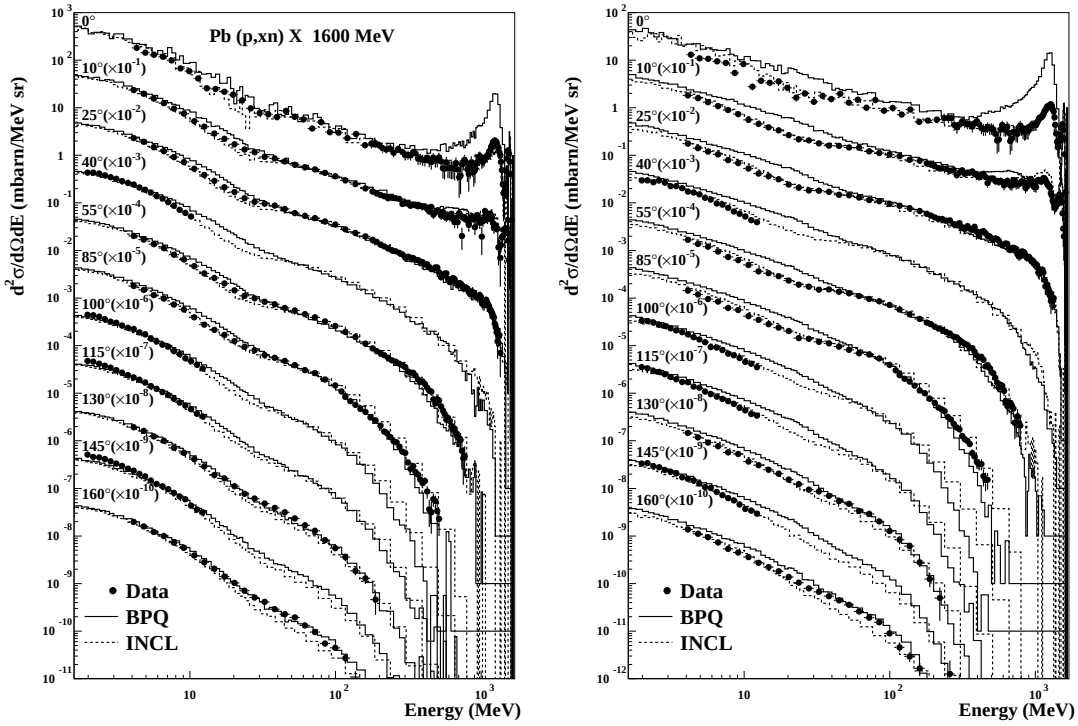


**Figure** 3: *Id. fig. 2 but for p (1600 MeV) + Pb (left) and Fe (right).*

## 3.2 Inferred average neutron multiplicities

Because the double-differential cross-section data nearly cover the full angular range with sufficiently close measurements, it was also possible to infer from the data average neutron multiplicities per reaction above the energy threshold of the detectors [2]. In figs. 4 and 5 the obtained experimental values as a function of respectively the mass of the target and the incident energy, for two different neutron energy ranges, are compared with the neutron multiplicities given by the two codes, TIERCE-INCL2 and LAHET-BPQ. This confirms in a rather synthetical way what has been discussed above. In all cases, INCL2 agrees with the data within the error bars while BPQ tends to overpredict 2-20 MeV neutron multiplicities, i.e. evaporation neutron production, especially at 1200 and 1600 MeV. For high energy neutrons (above 20 MeV) the sensitivity to the models is less important. This arises likely because of compensating effects, BPQ predicting more intermediate energy neutrons because of pre-equilibrium while INCL2 spectra often extend to higher energies. However, a significant deviation from the experiment is found at the highest energy (fig. 5 for iron with BPQ. It should be noticed that the relative contribution of high energy neutrons to the total multiplicity is much larger for light targets than heavy ones.

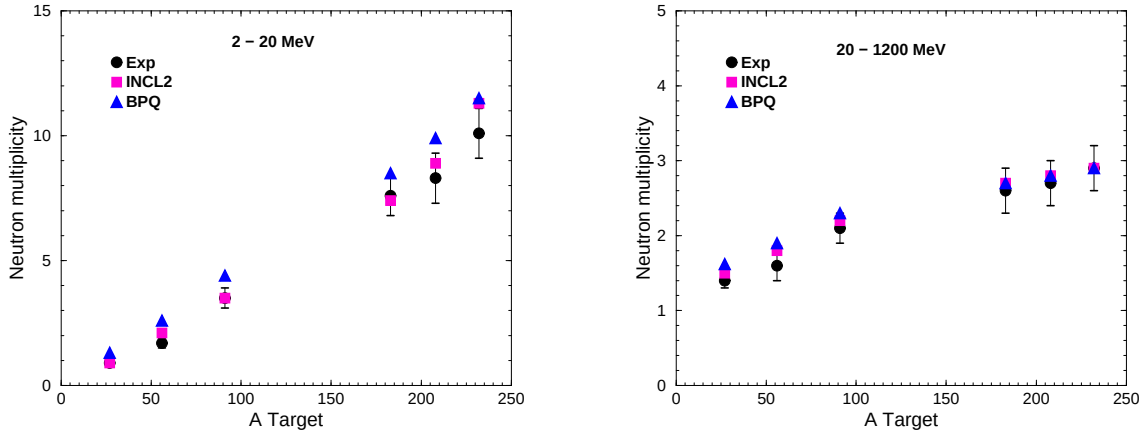


**Figure** 4: *Average neutron multiplicities per primary reaction inferred from the SATURNE double-differential cross-sections at 1200 MeV for the different targets. Left: [2-20 MeV] neutron multiplicities; Right: [20 MeV-Einc] neutron multiplicities. From [2].*

In [2] are also shown the average kinetic energies carried away by the neutrons, extracted from the energy weighted double-differential cross-sections (i.e. multiplied by neutron energy) using the same procedure as for the multiplicities were compared with the calculations. For the 2-20 MeV bin, conclusions similar to what was stated for multiplicities were drawn, reflecting the fact that Ex$M_n$ is governed by $M_n$ as far as the same evaporation model is used in both calculations and thus gives an identical energy spectrum for the low energy neutrons. For the high energy bin, the compensating effect noticed for the multiplicities seems to be even stronger and, regarding the uncertainties, it was not possible to discriminate both models. It is interesting, nevertheless, to remark that these high energy neutrons carry out the major part (from 80% for Th to 98% for Al) of the emitted neutron energy and a large amount (about 30%) of the incident proton energy. In a thick target this will play an important role in the spatial distribution of the energy deposition and particle production.

In summary, we can conclude that INCL2, once renormalized to obtain the correct total reaction cross-section, is able to globally reproduce the bulk of the data, with some slight discrepancies in the angular distributions. The Bertini model followed by pre-equilibrium, although it is found to be an improvement compared to Bertini alone, works perfectly for Pb at 800 MeV but fails as the energy is increased and the target gets lighter. ISABEL, tested only at 800 MeV, gives a similar agreement as INCL2 for Pb but a less good one for Fe.

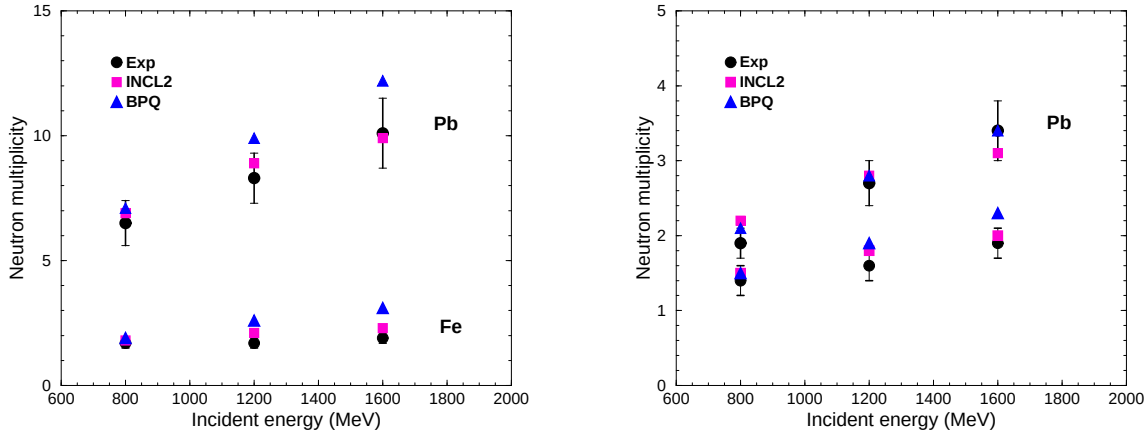


**Figure** 5: *Average neutron multiplicities per primary reaction inferred from the SATURNE double-differential cross-sections for Pb and Fe as a function of incident energy. Left: [2-20 MeV] neutron multiplicities; Right: [20 MeV-Einc] neutron multiplicities. From [2].*

# 4 Neutron multiplicity distributions

Neutron multiplicity distributions have been measured by the NESSI collaboration on really thin targets [4] and, amongst others, for cm thick targets [3, 18] that are similar to the ones used for double-differential cross-section measurements at SATURNE. However, in the NESSI experiments the measurements of the kinetic energy of the neutrons was not possible and the detector is mainly sensitive to low energy (below 20 MeV) neutrons while at SATURNE the detection threshold was between 2 and 4 MeV. This makes the comparison not straightforward.

## 4.1 cm thick targets

The comparison of the mean neutron multiplicities measured by NESSI and at SATURNE at 1200 MeV on 1 cm (resp. 2 cm) thick W and Pb targets was made in [2] and in D9. It is not very easy because of the respective threshold, efficiency of the detectors and diameter difference, but, after corrections to make the data comparable, it can be concluded that the two results are compatible within the error bars, as shown in fig.4. However, there is a tendency for the NESSI multiplicities to be slightly larger that the ones obtained from the double-differential cross-section integration.

Table 1 [3] shows the average neutron multiplicities $\langle M_n \rangle$ measured for 2 cm thick Pb and 1 cm thick W targets at different energies and calculated taking into account the detection efficiency. Calculations were done with LAHET and HERMES using in both cases

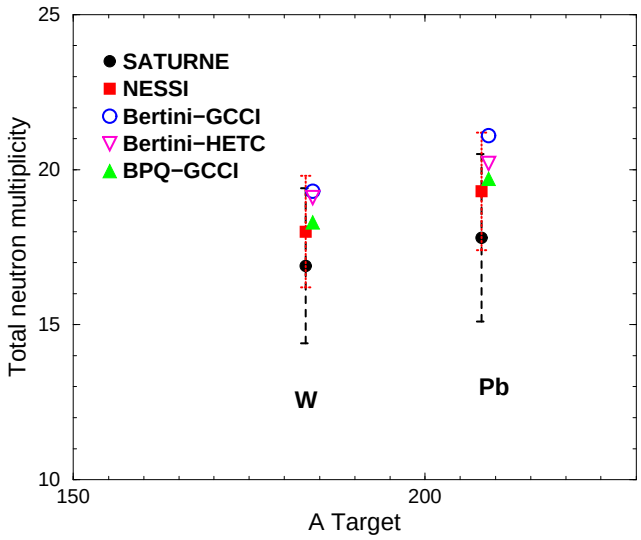


**Figure** 6: *Experimental average total neutron multiplicities per primary reaction for 15 cm diameter, 2cm thick Pb and 1 cm thick W targets from SATURNE (extrapolated from 3 to 15 cm diameter) and NESSI (corrected by detector efficiency and secondary reactions in the liquid scintillator) compared to calculations using LAHET with the Bertini INC and the GCCI level density parameterization in the Dresner-Atchison evaporation model (open circles), Bertini and the original HETC level density parameterization (open triangles) or adding a pre-equilibrium stage between INC and evaporation with GCCI (full triangles). For the sake of clarity the calculation symbols have been slightly shifted.*

the Bertini INC (without pre-equilibrium) and Dresner-Atchison evaporation-fission model with the original HETC level density parameterization. In the case of the calculations, the average neutron multiplicities before detector efficiency $\langle M_n^c \rangle$ are also given. It can be seen that generally the experimental values are in a somewhat better agreement with simulation calculations using HERMES than LAHET. The difference between LAHET and HERMES is not fully understood but likely originates from differences in the parameters of the evaporation model. However, there are systematic trends in quality of the agreement between calculations and data. In particular for the higher proton energy, theoretical calculations predict slightly higher average multiplicities than experimentally observed. Discrepancies seem to become larger for even higher energies [20]. The origin of these trends is presently not fully understood. Since high neutron multiplicities are essentially due to evaporation, overestimation of the neutron multiplicities by the models may be caused by an overestimate of the nuclear excitation energies as will be discussed in sect. 4.4 or too high Coulomb barriers (cf. sect. 4.5). In [3] it is also observed that the codes are also unable to reproduce the experimental data in the low-multiplicity region representing peripheral reactions. In this low $M_n$ region both codes appear to overestimate the probabilities especially for the 2.5 GeV

Table 1: *Average neutron multiplicities $\langle M_n \rangle$ for cylindrical 2 cm thick Pb and 1 cm thick W targets of 15 cm diameter bombarded with protons of different energies measured and calculated taking into account the detection efficiency with HERMES and LAHET. In the case of the calculations the average neutron multiplicities before detector efficiency $\langle M_n^c \rangle$ is also given. From [3].*

| Target | energy | LAHET | | HERMES | | Experiment |
|---|---|---|---|---|---|---|
| | | $\langle M_n \rangle$ | $\langle {M_n}^c \rangle$ | $\langle M_n \rangle$ | $\langle {M_n}^c \rangle$ | $\langle M_n \rangle$ |
| Pb | 1.2 GeV | 15.1 | 21.0 | 14.6 | 20.3 | 14.5 |
| Pb | 1.8 GeV | 18.9 | 26.5 | 18.0 | 25.3 | 17.7 |
| Pb | 2.5 GeV | 22.3 | 31.7 | 21.3 | 30.3 | 19.4 |
| W | 1.2 GeV | 16.3 | 22.2 | 15.0 | 20.5 | 14.8 |
| W | 1.8 GeV | 20.6 | 28.3 | 18.8 | 25.9 | 17.9 |
| W | 2.5 GeV | 24.9 | 34.2 | 22.8 | 31.7 | 20.5 |

incident proton energy. On the one hand the experimental precision for low neutron multiplicities is limited by threshold effects and accuracies in background corrections and on the other hand the description of the nuclear density profile of the nucleus has a large influence on the distributions for low $M_n$.

For the Pb target the deviation of theoretical predictions with respect to experimental data increases with increasing incident energy. The maximum discrepancies are found at 2.5 GeV, namely 13 (9.1) % for $\langle M_n \rangle$ for LAHET (HERMES). Note that the divergence for even higher incident proton energies (4.15 GeV) [20] still increases. Observations similar to those for lead were made for the tungsten target. At 1.2 GeV, agreement with experimental data is very good for the HERMES calculations, while it is still quite satisfactory for the LAHET calculations. However, for higher incident energies, the data clearly favor HERMES over LAHET calculations. At 2.5 GeV, deviations of the LAHET multiplicity distributions from the experimental data are quite substantial (17.6 %).

## 4.2 Sensitivity to the level densities and pre-equilibrium

In the case of the lead target bombarded by 1.2 GeV protons, a study of the sensitivity of the predictions to the level densities used in the evaporation model and to the adding of a pre-equilibrium stage was performed. The Gilbert-Cameron-Cook-Ignatyuk (GCCI) level densities instead of the original HETC ones were used (see [3]) and preequilibrium model was turned on in LAHET. Average multiplicities, $\langle M_n \rangle$ obtained from these studies are respectively 16.0 and 14.9 compared to 15.1 for the previous calculation. In LAHET, for Pb, the use of the GCCI level density parameterization tends to give higher mean multiplicities

than the experimental values. Such excess may result from an underestimate of the system temperature, related to the level density parameter, $a$, which in HETC is $a = A/10$ while it tends to $a = A/8$ in GCCI (see [3]). The same effect is illustrated in fig.4 for the multiplicities corrected for compatibility between SATURNE and NESSI, in which both Pb and W are shown. For W, the level density parameter in HETC being a=A/8 like in GCCI, no difference is seen. For the same level densities (here with GCCI), when an intermediate preequilibrium stage is introduced between INC and evaporation, neutron multiplicities are reduced on average by about one unit for both W and Pb targets. This is so, because particles from the preequilibrium stage have on the average higher kinetic energies than thermal particles reducing thermal excitation energies and, hence, average multiplicities. In addition, the low-multiplicity events associated with peripheral reactions are somewhat better described, when the preequilibrium stage is included in the calculations (not shown here). In general, improved agreement between experimental data and theoretical predictions is achieved when the preequilibrium model is used together with the GCCI description, as noticed also for the SATURNE results. Note that in the LAHET code the recommended and default parameter setting is indeed the GCCI option and pre-equilibrium switched on. However, to allow for a direct comparison of similar physics models in HERMES different options for LAHET had been choosen in this section.

## 4.3 Thin targets

Neutron multiplicity distributions have also been measured on a large variety of really thin targets at 1200 MeV [4]. In fig.7 the measured distributions are compared to calculations made with INCL2 coupled to the GEMINI [21] evaporation model after folding with the detector efficiency (shaded area). The dashed curve shows the distribution before taking into account the detector efficiency. It can be seen that generally the INCL2 calculations agree very well with the measured distributions. For heavier targets and low neutron multiplicities there exists however a discrepancy between experiments and calculations. A similar discrepancy was reported previously [20] and was ascribed to the sharp cut off modeling of the nuclear density distribution in INCL2.

## 4.4 Excitation energy distributions

From the preceeding sections, it is clear now that using Bertini-like intra-nuclear cascade codes leads to too large excitation energy. In fact, with Bertini one obtains thermal excitation energy distributions in the residual nuclei after INC which are extending towards larger values than the distributions of the INCL2 and ISABEL calculations do for the very same incident proton energy—as demonstrated in Fig. 8. This can be confronted directly

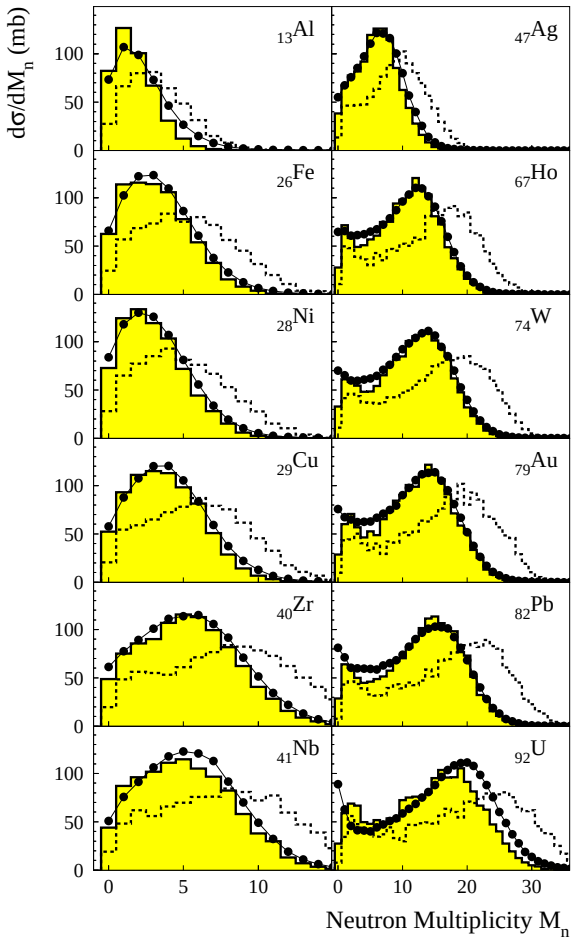


**Figure** 7: *Experimental (solid points) and calculated (histograms) mean neutron multiplicities as a function of the target atomic number $Z_T$ at 1.2 GeV. The calculated distributions are shown before (dashed line) and after (shaded area) folding with the detector efficiency. From [4].*

to the NESSI data since neutron multiplicities can be converted (provided that a formalism described in [24] is applied) into excitation energy. ISABEL and INCL2 calculations have been renormalized to the reaction cross-section of 1688 mb (p+Au) which is widely independent of incident proton kinetic energy. No pre-equilibrium option has been applied. For thermal excitation energies larger than some 10 MeV and incident proton energies up to 1.2 GeV, the ISABEL code coincides with the INCL2 predictions. For incident proton energies larger than 1.2 GeV, the validity range of ISABEL is exceeded [8] and consequently $\mathrm{d}\sigma/\mathrm{d}E^*$ distributions for 2.5 GeV are not shown in Fig. 8.

The different cross-sections $d\sigma/dE^*$ at low $E^*$ caused essentially by peripheral collisions can, among other things, be explained by differences in the nuclear density description of the nuclei. Probably the 16 step approximation of the nuclear density in the ISABEL code

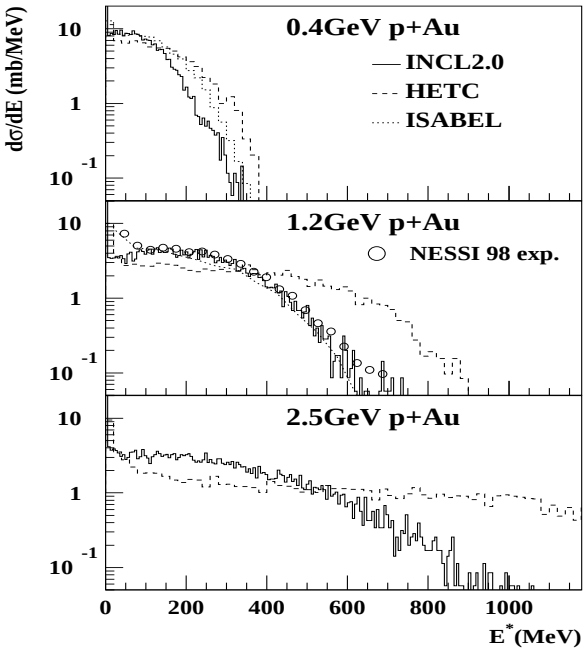


**Figure** 8: *Thermal excitation energy $E^*$-differential cross-sections for 0.4, 1.2 and 2.5 GeV p+Au reaction following calculations with HETC (Bertini-like, dashed histogram), the INCL2 (solid curve) and the ISABEL code (dashed-dotted line). For 1.2 GeV deduced $E^*$ distributions of the NESSI experiment (∘) [23] are also plotted. From [3].*

is responsible for the enhancement of $d\sigma/dE^*$ at low $E^*$ as compared to the other models. When confronting $d\sigma/dE^*$ with experimental distributions [23] the INCL2 and ISABEL code coincides almost perfectly for both light (Fe) and heavy (Au) targets (Fig. 8) while Bertini based codes overestimate $d\sigma/dE^*$ at high $E^*$, particularly for heavier targets. As e.g. compared to the 1.2 GeV p+Au experiment the average $E^*$ is overrated by 110–140 MeV. ISABEL shows extremely nice agreement with experimental distributions even at low $E^*$ for the reason just mentioned above.

Actually only a small part (approximately 1/10 to 1/5—depending on the nucleus, the incident energy, and the codes used) of the total available energy (incident kinetic energy of the proton) can be converted into thermal excitation energy. The remaining part is carried off by highly energetic nucleons and mesons during the fast INC. On the average for large incident proton energies the Bertini codes predict almost a factor of two higher $E^*$ values than INCL2 does. The considerable deviation between Bertini on one hand and INCL2/ISABEL on the other hand for higher $E^*$ is all the more pronounced as the energy of the incident proton increases. One assertion which could explain the disagreement is the way the originally transferred energy is being exhausted or carried away by the different exit particles. While the INCL2 code predicts many relatively highly energetic particles during

the INC, the HETC codes (LAHET or HERMES) produce not only fewer, but also less energetic $\pi^{\pm}$ and $\pi^0$ following the reaction 1.2 GeV p+Au. The appraisement of the quality of pion spectra and production cross-sections $\sigma_{\pi}^{\text{total}}$ is however difficult due to the lack of experimental data in the energy regime beyond 1 GeV.

## 4.5 Influence of the Coulomb barriers on production cross-sections

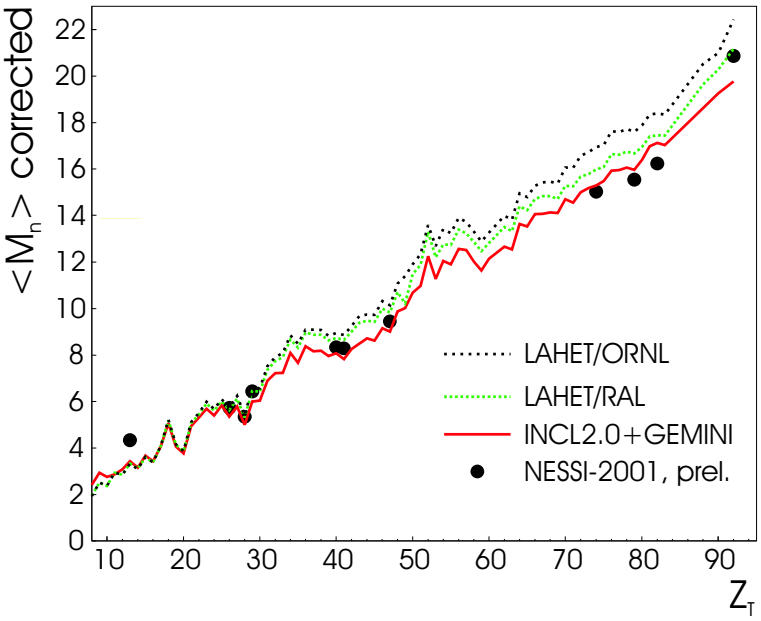


**Figure** 9: *Measured, after correction by the detector efficiency, (solid points) and calculated (lines) neutron multiplicity distributions for different thin targets at 1200 MeV. The dashed (resp. dotted) lines are obtained by LAHET calculations using the Bertini INC followed by Dresner with ORNL (resp. Atchison (RAL)) fission model. The solid line is given by the INCL2+GEMINI model combination. From [4]*

By default LAHET and HERMES HETC exert the Dresner-Atchison fission/evaporation code which on its part reduces the Coulomb barriers with increasing $E^*$. It has been found (see WP4) that the production cross-sections for H (all targets) and He isotopes (for heavy targets) are generally overestimated by a factor of approximately two for Bertini based codes (HERMES, LAHET using Dresner-Atchison evaporation/fission model), while the INCL2 code coupled to the statistical evaporation model GEMINI [21] gives reasonable agreement with the NESSI experimental data [23]. Actually this has been interpreted [22] by the fact that, the Coulomb barriers being considerably smaller in LAHET than in GEMINI: both because they are smaller at E*=0 and because in Dresner-Atchison, they decrease whith increasing E*. The latter effect being amplified by the fact that Bertini gives a larger E* than INCL2. In [3] the effect of the scaling down of barriers with excitation energy was tested by, in the LAHET code system, applying the ORNL fission/evaporation formalism which

does not contain the scaling down of the Coulomb barriers with $E^*$. It was found that the H (except proton) and He-production cross-sections are then reduced drastically, the proton not being much affected. Actually, a considerable feedback on the neutron kinetic energy spectra and multiplicities is caused by the variation of the Coulomb barriers applied in the evaporation codes, because changing the emission width for charged particles effects at the same time the emission probability for neutrons, the two emissions being in competition. The influence of modifying the Coulomb barriers on the $M_n$ is demonstrated in Fig. 9 for 1.2 GeV proton induced reactions on the different thin targets. It can be seen that, for the same excitation energy at the end of the cascade (Bertini), $M_n$ is larger when the Coulomb barriers is kept constant (LAHET-ORNL dashed line) than when it is reduced with $E^*$ (LAHET-RAL dotted line). The INCL2-GEMINI calculation for which the excitation energy is lower and the barrier similar to the ORNL case gives an even lower multiplicity closer to the experimental values. This problem of too low Coulomb barriers in the Bertini-Dresner model was also suspected as the cause of its bad predictions of the isotopic distributions measured at GSI [17].

# 5 Conclusion

In this report, we have made a comprehensive comparison of the whole set of thin target data collected within WP5 with some of the high energy models commonly used in high energy transport codes for applications. It has been shown that the combination of the Bertini-Dresner-Atchison models, which is the default option of most of the codes, presents serious deficiencies, although less important when used in the HERMES package. It is clear that the Bertini INC predicts too large excitation energy at the end of the cascade stage, therefore overestimating, especially at high incident energies, the number of evaporated neutrons. The adding of a pre-equilibium stage improves the prediction of the code, in particular for low energy neutron multiplicities. However discrepancies tend to remain for neutrons produced at intermediate kinetic energy for high incident energies and grow larger as the target becomes lighter. The ISABEL model was also tried, when possible, and was found to give a good agreement with both the double-differential cross-sections and the multiplicity distributions. Only for iron, the predictions were less good. Finally, we have shown that the use of the Cugnon intranuclear cascade model, INCL2 is able to fairly reproduce the whole bulk of our results. However, it should be recalled that this model still suffers from serious deffects mostly due to the fact this it does not treat correctly the diffuseness of the nuclear surface. This obliges to renormalize the calculations to the correct total reaction cross-section. Also, it makes it impossible to have a correct prediction of the most peripheral collisions. The new version of the Cugnon model, INCL4 [25], under progress in WP8 is expected to solve this

problem. The influence of the level density parameterization and Coulomb barriers (which are suspected of being too low in the Dresner-Atchison model to predict charged particle and residue data) was also tested and found to have an influence on the neutron multiplicities. The ABLA evaporation-fission model [26] also under development in WP8 is intended to give better level densities and Coulomb barriers.

# References


[1] X. Ledoux et al., Phys. Rev. Lett. **82**, 4412 (1999).

[2] S. Leray et al., Phys. Rev. **C65**, 044621 (2002).

[3] D. Filges et al., Eur. Phys. J. **A11**, 467 (2001).

[4] C.M. Herbach et al., FZJ Jülich annual report (2001).

[5] T. W. Armstrong and K. C. Chandler, HETC Monte-Carlo Nucleon-Meson Transport Code, Report CCC-178, ORNL(1977) and Nucl. Sci. Eng. **49**, 110 (1972).

[6] G.Sterzenbach et al., 2nd Int. Topical meeting on nuclear Application of Accelerator Technology, AccApp98', ISBN 0-89448-633-0, Sep. 20–23, Getlinburg (1998).

[7] P.Cloth et al., HERMES, Report Jülich 2203, ISSN 0366-0885, (1988).

[8] R.E.Prael and H.Liechtenstein, Report LA-UR-89-3014 Los Alamos National Laboratory (1989).

[9] O. Bersillon, *2nd Int. Conf. on Accelerator Driven Transmutation Technologies*, Kalmar, Sweden, June 3-7, 520, (1996).

[10] H. W. Bertini et al., Phys. Rev. **131**, 1801 (1963).

[11] L. Dresner, Oak Ridge report ORNL-TM-196 (1962)

[12] F.Atchison, Intermediate Energy Nuclear Data: Models and Codes, Proc. of a Specialists' Meeting, OECD/NEA, Issy-le-Moulineaux, France, May 30 - June 1 (1994) 199.

[13] Y. Yariv and Z. Fraenkel, Phys.Rev. **C20** (1979) 2227; Y. Yariv and Z. Fraenkel, Phys.Rev. **C24** (1981) 448.

[14] J. Cugnon, Nucl. Phys. **A462**, 751 (1987); J. Cugnon, C. Volant and S. Vuillier, Nucl. Phys. **A620**, 475 (1997).

[15] R. Prael, private communication.

[16] J. Cugnon et al., Phys. Rev. **C56**, 2431 (1997).

[17] W. Wlazlo et al., Phys. Rev. Lett. **84**, 5736 (2000).

[18] A. Letourneau, Nucl. Instr. and Meth. in Phys. Res. **B170** (2000) 299.

[19] D.Hilscher et al., Nucl. Inst. and Meth. **A414**, 100 (1998).

[20] L. Pienkowski et al., Phys. Rev. **C56**, 1909 (1997).

[21] R.J.Charity et al., Nucl. Phys. **A483**, 371 (1988).

[22] D.Hilscher et al., J. Nucl. Mat. **296**, 83 (2001).

[23] M. Enke et al., Nucl. Phys. **A657**, 319 (1999).

[24] F.Goldenbaum et al., Phys. Rev. Lett. **77**, 1230 (1996).

[25] A. Boudard et al., Phys. Rev. **C66** 044615 (2002).

[26] A. R. Junghans, M. de Jong, H. G. Clerc, A. V. Ignatyuk, G. A. Kudyaev and K.-H. Schmidt, Nucl. Phys. **A629**, 635 (1998) and K.H. Schmidt et al., work in progress.